Int. J. Electrochem. Sci., 11 **(2016)** 2046 - 2057

International Journal of
ELECTROCHEMICAL
SCIENCE
www.electrochemsci.org

Short Communication

Preparation of Pt/C Catalyst with a Novel Solid Phase Reaction at Room Temperature and its Electrocatalytic Active for Methanol Oxidation

Yunshan Bai[1,2,*], *Lude Lu*[2], *Jianchun Bao*[2]

[1] College of Chemistry and Chemical Engineering, Yancheng Institute of Technology, Yancheng 224051, P. R. China
[2] Key Laboratory for Soft Chemistry and Functional Materials of Ministry of Education, Nanjing University of Science and Technology, Nanjing 210094, P. R. China
[*]E-mail: ysbai_njust@163.com, bys@ycit.edu.cn

Received: 31 October 2015 / *Accepted:* 23 December 2015 / *Published:* 1 February 2016

Pt/C catalyst was prepared by novel solid phase reaction method for the first time. Firstly, the Vulcan XC-72 active carbon powder, H_2PtCl_6 solution and NaOH solution were mixed, ground and dried under vacuum to completely remove solvent. Then, the mixture was ground for hours, filtered and washed. The electrode materials were characterized by XRD and TEM. The results demonstrated that the Pt/C catalyst prepared by solid phase reaction method had low crystallinity and small particle size. Under the three electrode test system, the electrochemical properties of catalyst were measured cyclic voltammetry, current-potential polarization curves, *et.al*. Besides, its performance was compared with that of the commercial E-TEK Co Pt/C catalyst and Pt/C catalyst prepared by traditional liquid phase reaction method. The results show that the electrocatalytic activity of Pt/C catalyst prepared by solid phase reaction was higher than that of the commercial E-TEK Co Pt/C catalyst and the Pt/C catalyst prepared by traditional liquid phase reaction method.

Keywords: Solid phase reactions, fuel cell, Pt/C catalyst

1. INTRODUCTION

Fuel cell is a kind of energy device which can convert chemical energy into electric energy by catalytic reaction. In theory, as long as the fuel and oxidant are constantly added, it has unlimited power generation capacity [1]. At present, hydrogen [2], methanol [3], formic acid [4] and ethanol [5], et.al has been usually used as fuel. Direct methanol fuel cell (DMFC) has developed rapidly due to the virtues of simple structure, low cost of liquid fuel and high theoretical energy density. Methanol fuel is widely available with safe storage, so it is easy to operate. These attractive properties make it more likely to replace the hydrogen fuel cell and the charging power supply [6].

The carbon supported PtM (M = Ru [7-11], Pd [12], Sn [13-14], Os [15], Ir [16], et al.) catalysts have been recognized as the best metal catalyst for the methanol oxidation reaction (MOR). The activate carbon supported metal catalyst was generally prepared by gas phase reduction reaction (GPR) and liquid phase reduction reaction (LPR). In the most typical GPR method procedure, the precursor of Pt compounds loaded on high surface area supports was reduced by H_2 [11, 17-19]. Frelink et al [17] prepared activated carbon supported Pt catalyst with Pt particles size of 7.80 ± 2.5 nm through the reduction of H_2PtCl_6 by H_2 at 700 ^oC for 2 h. Takasu et al. [11] and Rauhe et al. [18] obtained PtRu/C catalyst by co-deposition of metal chlorides precursors onto high surface area graphite, followed by reduction in a hot H_2/N_2 stream. Compared with GPR, LPR method is more common adopted in the preparing of PtM/C catalyst. There have been large numbers of reports about the preparation of PtM/C catalysts with various reductant (such as: $NaBH_4$ [20,21], $Na_2S_2O_4$ [22], hydrazine [23], organic acids [24], alcohols [25,26], aldehyde [19], sugars [19], et al.) to reduce the Pt precursor compounds loaded on high surface area supports.

The preparation method and preparation process of catalyst show a great influence on its performance. GPR, LPR method has the advantages of convenient and feasible while the disadvantage is the poor dispersity, especially the uneven distribution of each component often occurs inside the carrier under multiple components conditions. The velocity of molecular motion in solid phase system is far less than that of liquid phase. The nascent state platinum particles adsorbed on the activated carbon is not easy to further growth, which is beneficial to the formation of ultrafine particles, and is also advantageous to the formation of a defective crystal or amorphous material. Thereby, the specific surface area and the number of active centers of the catalyst are increased, showing excellent catalytic performance to the electrocatalytic oxidation of methanol or hydrogen.

In this paper, we reported the preparation of Pt/C catalyst with a novel solid phase reaction method (SPR) at room temperature. The morphology and particle size of the catalysts were analyzed by X-ray diffraction (XRD) and transmission electron microscopy (TEM). The effect of the preparation conditions on the activities of the Pt/C catalysts for the methanol oxidation reaction was also studied.

2. EXPERIMENTAL

2.1. Preparation of the catalyst

Vulcan XC-72 carbon black (E-TEK) was mixed with H_2PtCl_6 solution and NaOH solution. The mixture was completed dried under vacuum. After cooling to room temperature, a litter polyformaldehyde were added to the system as solid reductant and the resulted mixture was abraded for 2-3 h. Then, the sample was washed with water until no chlorine ions were detected and then dried under vacuum at about 50 °C. The Pt metal load amount in the Pt/C catalysts is 20 wt.%. The obtained catalyst was marked as Pt/C (SPR).

For comparison, traditional LPR method was adopted with $NaBH_4$ as reductant. 100 mg Vulcan XC-72 carbon black was mixed with 4 mL absolute alcohol and 3.25 mL H_2PtCl_6 aqueous solution. Under room temperature, 2 mL 0.1 mol L^{-1} $NaBH_4$ aqueous solution was added to the above system. One minute latter, 0.4 mL 6 mol L^{-1} HCl was added to the solution to decompose excess $NaBH_4$. After

filtrated and washed, Pt/C catalyst was obtained in which Pt load amount is also 20 wt %. The obtained catalyst was marked as Pt/C (LPR).

For comparison, Pt/C catalyst (the catalyst of E-TEK Co..) in which Pt is also 20 wt %.

2.2 Preparation of the Membrane electrode

The thin film electrodes were prepared using the method reported by Schmidt et al. [27]. Glassy carbon electrode (4 mm diameter) was polished to mirror before each experiment. By ultrasonically dispersing and mechanical stirring, 10 mg Pt/C catalyst was dispersed in 5 mL H_2O. The 8.8 μL suspension was pipetted onto the surface of glassy carbon. After the evaporation of H_2O, the 8.8 μL Nafion solution (5 wt %) was sprayed on the surface of Pt/C catalyst. The Pt loading was 28 $\mu g/cm^2$ and the thickness of Nation film is 0.2 μm.

2.3 Electrochemical performance studies

The electrochemical measurements were performed with CHI 600 potentiostate (CHI Co.) and a traditional three-electrode cell. Pt/C catalyst modified glass carbon electrode was used as the working electrode. The saturated calomel electrode (SCE) and Pt plate were used as the reference and auxiliary electrode, respectively. The solution used for the electrochemical measurements was 0.5 mol L^{-1} H_2SO_4 or 0.5 mol L^{-1} CH_3OH + 0.5 mol L^{-1} H_2SO_4 solution. High-purity nitrogen was used for deaeration of the solution before measurements. During the measurements, a gentle nitrogen flow was kept above the electrolyte surface. The cyclic voltammetry experiment was carried out at 298 K with the scan rate at 50 mV s^{-1}.

2.4 XRD and TEM

The surface morphology of different Pt/C catalysts was characterized by transmission electron microscopy (TEM) and X diffraction (XRD). TEM analysis was carried out by JEM-2100 transmission electron microscopy (JEOL) and the working voltage was set at 200KV. The magnification or scale was selected depending on the specific circumstances. XRD was carried out by D/MAX-rC X-ray diffractometer (Rigako, Japan) with Cu target K_α (λ = 0.1542 nm).

3. RESULTS AND DISCUSSION

3.1. Analysis of the morphology and the particle size

Fig.1 shows the XRD patterns of Pt/C (SPR), Pt/C (LPR) and the commercial Pt/C 20 wt. % from E-TEK. The characteristic diffraction peaks of Pt [111], [200], [220], [311] crystal face are clearly observed at 2 θ values of ca. 39.9, 46.5, 67.8, and 81.2^o, respectively. The 2 θ values correspond to the crystal plane diffraction peaks of Pt [111], [200], [220], [311] with a face centered cubic structure (JCPDS card 04-0802)[28], indicating that the crystal structure of the Pt particle in the Pt/C catalyst is surface centered cubic. The relative crystallinity of the catalysts was evaluated using

the method reported by Antolini et al. [22] namely the bigger the peak height ratio of the Pt[111] crystal face and the reflexion of the carbon, the higher the crystallinity. The average particle size can be estimated using Scherrer [22, 29] equation given as follows:

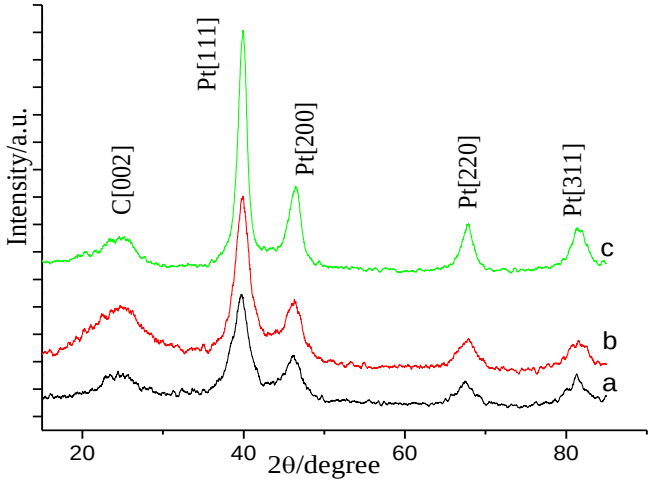

Figure 1. XRD pattern of the different Pt/C catalysts.(a)E-TEK, (b)SPR, (c)LPR.

$$d = 0.94\lambda / \beta_{1/2} \cos\theta \quad (1)$$

Where d is the average particle sizes (nm), λ the wavelength of X-ray radiation, θ the angle at the position of the peak maximum, $\beta_{1/2}$ the width of the diffraction peak at half height. Table 1 lists the calculated relative crystallinity and the average particle sizes for all the catalysts on the basis of the XRD patterns. It shows that the Pt particle average sizes in the Pt/C (SPR), Pt/C (LPR) and the catalyst of E-TEK are 3.77, 8.44 and 3.20 nm, respectively.

Although the particle size of Pt in the Pt/C catalyst of E-TEK was less than that of the Pt/C catalyst prepared by solid phase reaction, endowing the Pt in the Pt/C catalyst of E-TEK with larger specific surface area accordingly and larger electrochemical active area theoretically, Table 2 has shown no significant difference between the two catalysts. This result showed that there were more defects in the Pt surface in the Pt/C catalyst prepared by solid phase reaction method, which provided more active Pt atoms, leading to an increase in the electrochemical activity of the catalyst [30].

Table 1. The relative crystallinity and average particle size of the different Pt/C catalysts from XRD and TEM.

Catalyst	relative crystallinity	Particle size (nm,XRD)
SPR	2.38	3.77
E-TEK	2.70	3.20
LPR	5.56	8.44

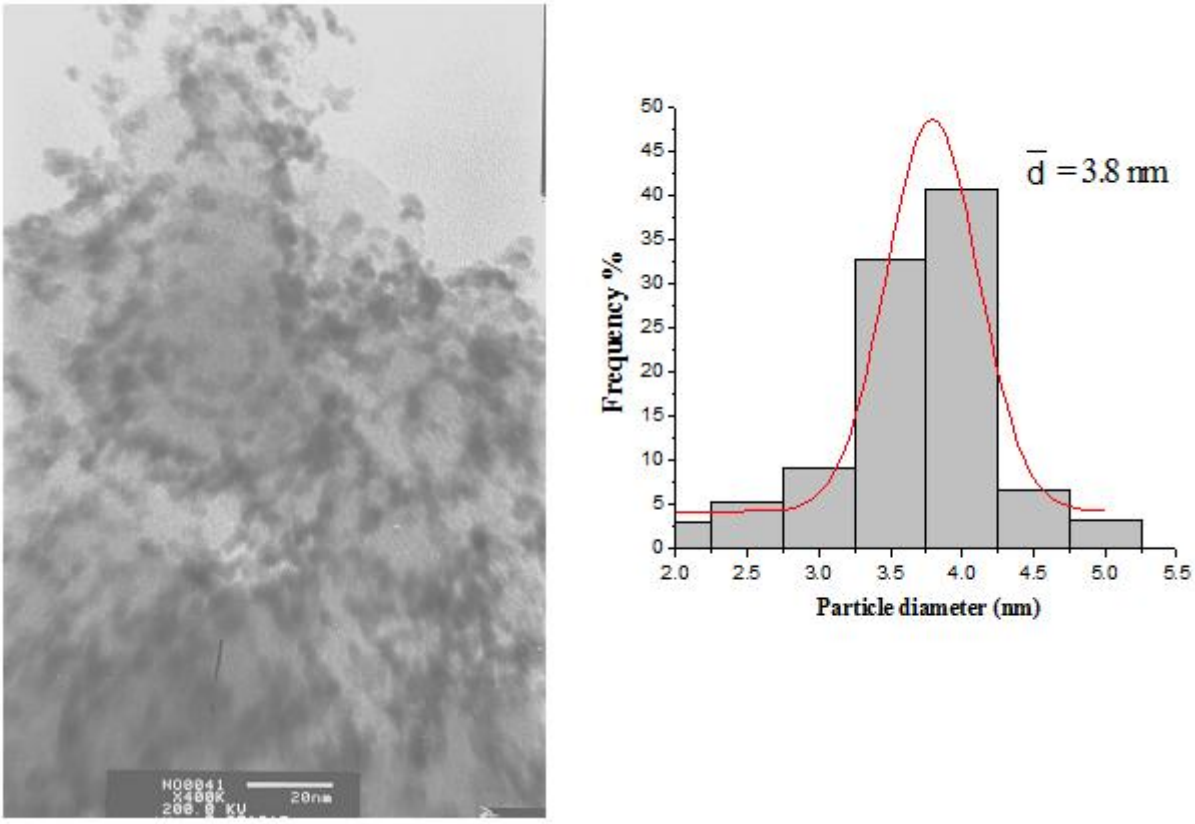

Figure 2. TEM images of the Pt/C (SPR) catalysts.

Meanwhile, the Pt/C (SPR) catalyst possessed lower crystallinity than the Pt/C (LPR) and the catalyst of E-TEK. It might be due to that the reactant molecules were homogeneous surrounded in solvent molecules in liquid system, and the collision opportunity of molecules is equal, facilitating the formation of crystalline state Pt particles. However, comparing with the valence Brownian movement in liquid phase system, the movement of molecules was very slow in solid phase system, profiting the formation of ultramicron.

There have been studies indicated that the size of Pt particles influenced the performance of catalysts for the MOR [17, 31-32]. Therefore, the Pt/C catalyst with largely uniform Pt metal particles was favorable to improve the catalytic activity for the MOR.

Fig. 2 shows the TEM images of the Pt/C catalysts prepared by the SPR method and the corresponding particles size distribution histograms. The results were in good agreement with the XRD data. As shown in Fig. 2, the Pt nanoparticles are well dispersed on the surface of carbon with a narrow particle size distribution. No any local conglomeration is found in the Pt/C (SPR) catalyst. It might be due to the different growth mechanism of the Pt particles for the SPR and the LPR system. In the SPR system, the Pt precursor compound loaded on active carbon was reduced through the solid-solid interfacial reaction, so the formation of Pt metal nanoparticles must again undergo a process of transfer, congregation, nucleation and growth. The process was very favorable to improve the dispersity and lower the size of Pt nanoparticles.

3.2 Comparing of the electrochemical activities

Fig 3 showed the cyclic voltammetry of Pt/C catalyst in 0.5 mol L^{-1} H_2SO_4 (a) SPR、E-TEK Pt/C catalyst, (b) E-TEK and the Pt/C catalyst prepared by liquid phase reaction, (c) LPR electrode. The redox peaks of Pt were observed in the three cyclic voltammetry curves. However, the redox peak potential for E-TEK Pt/C catalyst and Pt/C catalyst prepared by solid phase reaction were more negative than that of Pt/C catalyst prepared by liquid phase reaction while the peak current density of E-TEK Pt/C catalyst and Pt/C catalyst prepared by solid phase reaction were larger that of Pt/C catalyst prepared by liquid phase reaction, demonstrating that the Pt/C catalyst of E-TEK and the Pt/C catalyst prepared by solid phase reaction are more likely to be oxidized. The reason was that the Pt particles in the Pt/C catalyst of E-TEK and Pt/C catalyst prepared by solid phase reaction were with small sizes and easy to be oxidized [28] and this phenomenon was consistent with the particle size of Pt particles measured by XRD and TEM.

As shown in Fig 3, in the three cyclic voltammetry curves, redox peaks of hydrogen dissociation adsorption all appeared in -0.2V~0.05V potential region, with different peak currents. The redox peak current of hydrogen dissociation adsorption of E-TEK catalyst was similar to that of the Pt/C catalyst prepared by solid phase reaction, but it was much larger than that of Pt/C catalyst prepared by liquid phase reaction. This result indicated that the surface of Pt in E-TEK catalyst and Pt/C catalyst prepared by solid phase reaction was much larger than that of Pt/C catalyst prepared by liquid phase reaction, which was consistent with the particle size of Pt particles measured by XRD and TEM.

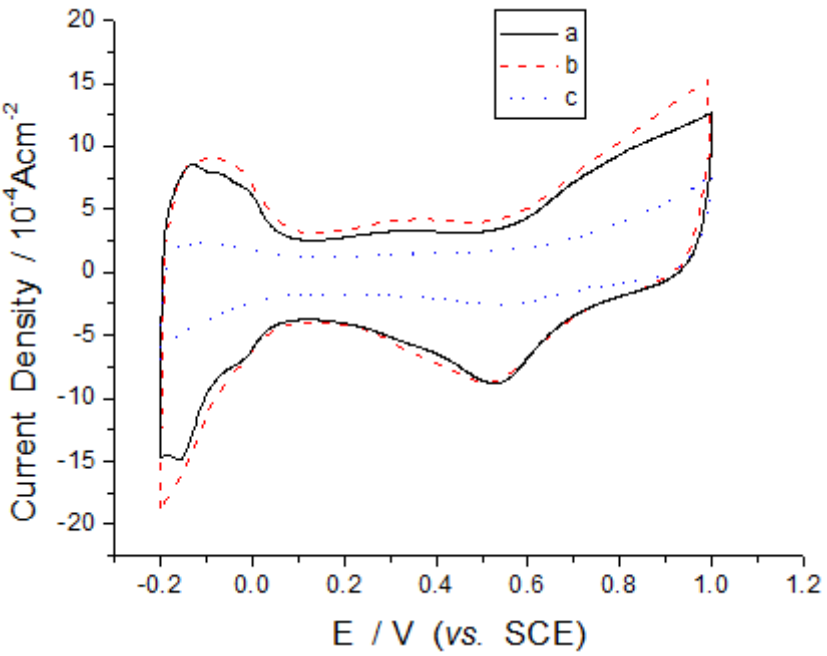

Figure 3. Cyclic voltammograms of the different Pt/C catalysts in 0.5 mol L^{-1} H_2SO_4. Scan rate 50 mV/s. (a)SPR, (b)E-TEK, (c)LPR.

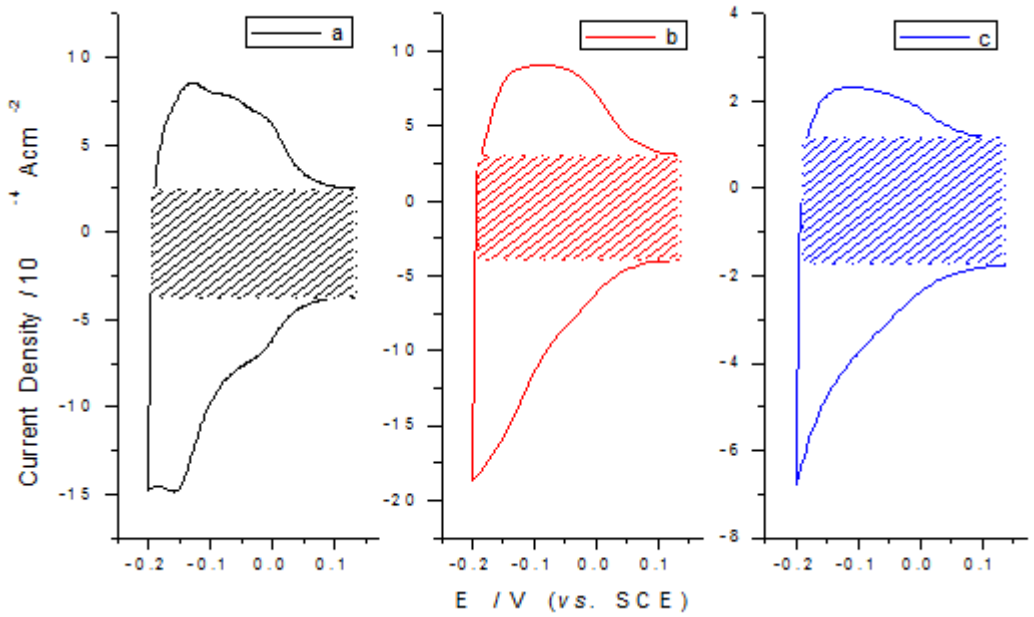

Figure 4. Hydrogen adsorption/desorption area in fig. 3. (a)SPR, (b)E-TEK, (c)LPR.

Fig. 4 shows the hydrogen adsorption/desorption region. The coulombic charge for hydrogen desorption (Q_H) was used to calculate the electrochemical active surface (EAS) by means of Eq.(2) [33] :

EAS ($m^2 g^{-1}$) = Q_H(mC)/ 0.21(mC cm^2) / Pt loading(mg) /10 (2)

where 0.21 represented the charge required to oxidize a monolayer of H_2 on bright Pt. The surface area of catalysts were calculated using Eq.(3) [33]:

$S = 6000/\rho d$ (3)

where S was the specific surface area ($m^2 g^{-1}$) and ρ was the Pt density (21.4g cm^{-3}) while d was the average particle sizes (nm). Table 2 lists EAS and the surface area of the different catalysts by Eq.(2) and Eq.(3). As shown, although the surface area of the Pt/C (SPR) catalyst was smaller than the E-TEK catalyst, its EAS catalyst was approximate to the E-TEK catalyst and much higher than that of the Pt (LPR). It illustrated that the surface of Pt/C (SPR) catalyst possesses more activity sites and results in the increase of EAS.

Table 2. Electrochemical active surface (EAS) and the specific surface area of the different Pt/C catalysts

Catalyst	EAS ($m^2 g^{-1}$Pt)	Surface area （$m^2 g^{-1}$ Pt）
SPR	36.1	73.78±9.71
E-TEK	35.6	87.61±5.48
LPR	8.60	31.16±4.54

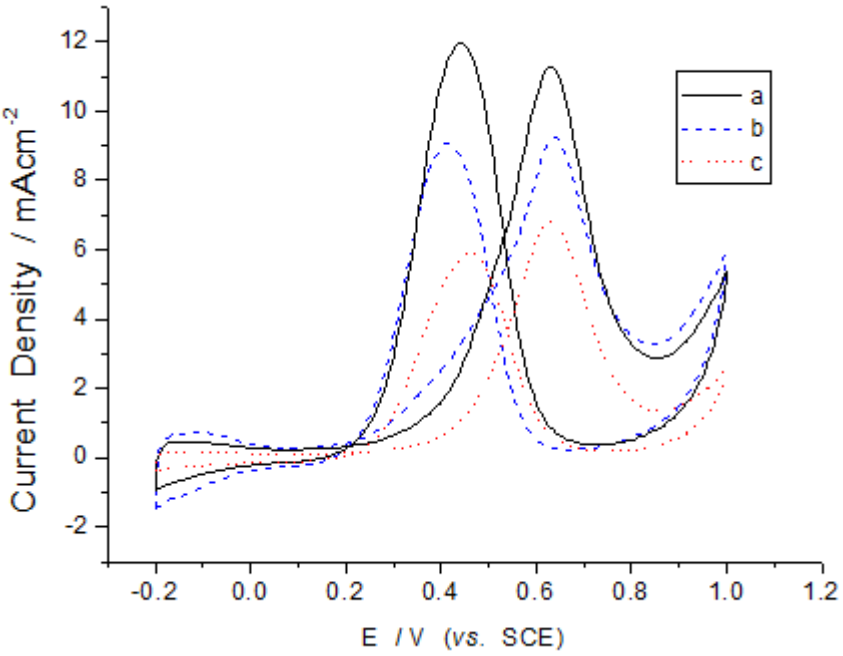

Figure 5. Cyclic voltammograms of the different Pt/C catalysts in 0.5 mol L^{-1} CH_3OH + 0.5 mol L^{-1} H_2SO_4. Scan rate 50mV/s. (a)SPR, (b)E-TEK, (c)LPR.

Fig.5 shows the cyclic voltammograms of the three catalysts in 0.5 mol L^{-1} CH_3OH + 0.5 mol L^{-1} H_2SO_4. The overall shape of the cyclic voltammetry of the sample was consistent with most literature and the typical methanol oxidation current peak of Pt catalyst was about 0.74 V vs. SCE [34-35]. The methanol oxidation peaks of the three samples were all located at about 0.64V and low anodic over potential of Pt/C catalyst showed higher electrocatalytic activity. For the positive scan, the oxidation peaks of methanol were all located at ca. 0.64V. However, the peak current density of the Pt/C (SPR) catalyst was 11.3 mA/cm^2, which was much higher than that of the Pt/C catalyst of E-TEK (9.7 mA/cm^2) and the Pt/C (LPR) catalyst (7.2 mA/cm^2). It demonstrated that the Pt/C (SPR) on the MOR possessed higher electrocatalytic activity. It might be due to that the Pt/C (SPR) catalyst processed more reasonable Pt particles size and lower crystallinity than the Pt/C (LPR) and the catalyst of E-TEK.

Fig. 6 showed the polarization curves of different Pt/C catalyst-Nafion membrane electrodes in CH_3OH (0.5 mol L^{-1}) + H_2SO_4 (0.5 mol L^{-1}). As shown, the open circuit potential was -0.07V for the Pt/C catalyst membrane electrode prepared by solid phase reaction, which was about 0.11V more negative than that of Pt/C catalyst membrane electrode prepared by liquid phase reaction. This result demonstrated that if single cell battery was assembled, the catalyst prepared by solid phase reaction could improve the open circuit voltage of the battery. Besides, the polarization performance of the Pt/C catalyst membrane electrode prepared by solid phase reaction was similar to that of E-TEK Pt/C catalyst membrane electrode, but was much better than that of Pt/C catalyst membrane electrode prepared by liquid phase reaction. The electrode potentials were 0.36, 0.36 and 0.80V respectively for the three membrane electrodes, when current density was 80mA/cm^2. When electrode potential was

0.4V, their current densities for methanol electro catalytic oxidation were 96.6, 94.8 and 14.4 mA/cm^2, respectively. The current density of Pt/C catalyst membrane electrode prepared by solid phase reaction method for methanol electrocatalytic oxidation was better than that of the reported value of 59.5 mA/cm^2 [3].

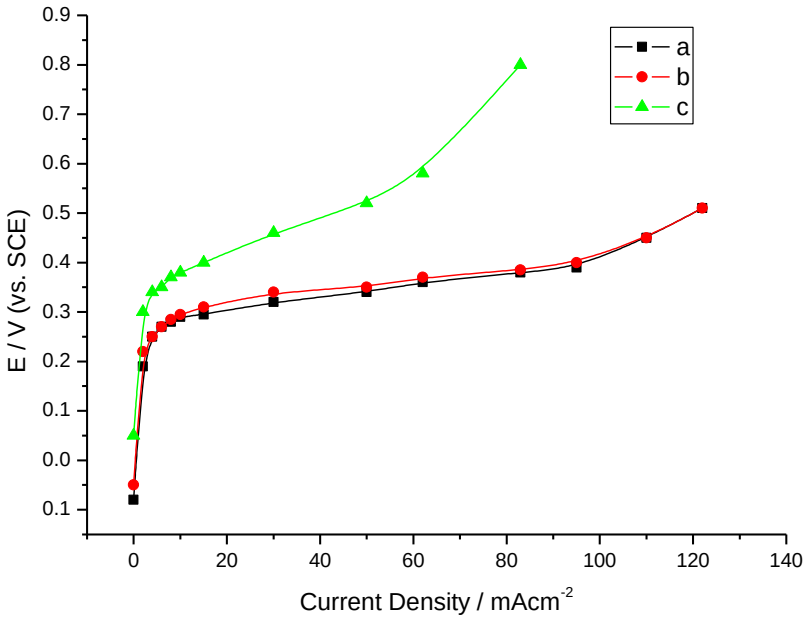

Figure 6. The polarization curves of different Pt/C catalyst-Nafion membrane electrodes in CH_3OH (0.5 mol L^{-1}) + H_2SO_4 (0.5 mol L^{-1}). (a)SPR, (b)E-TEK, (c)LPR.

3.3. The influence of the preparation conditions on the performance of catalyst

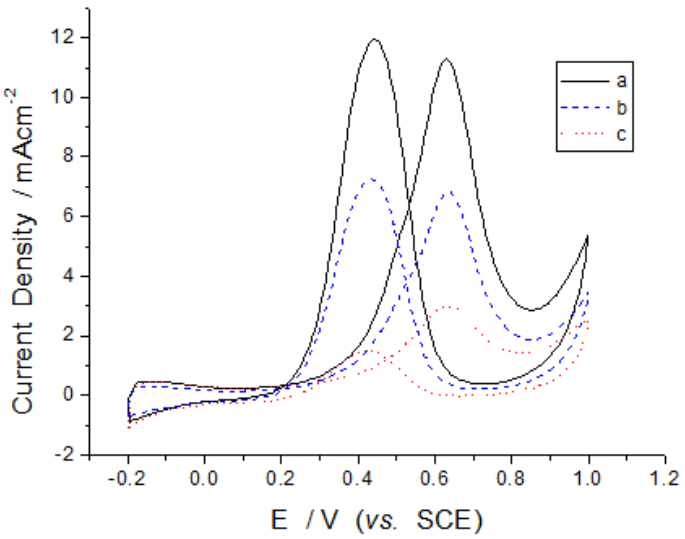

Figure 7. Cyclic voltammograms of the different Pt/C catalysts using (a) polyformaldehyde, (b) $NaBH_4$, (c) sodium formate as solid reductant in 0.5 mol L^{-1} CH_3OH + 0.5 mol L^{-1} H_2SO_4. Scan rate 50mV/s.

In order to further investigate the properties of the PtM/C catalyst, the influence of the preparation conditions on the performance of Pt/C catalyst was also discussed. Fig.7 showed the cyclic voltammograms of the different Pt/C catalysts prepared by using $NaBH_4$, sodium formate and Polyformaldehyde as reductant. Obviously, the Pt/C catalyst using polyformaldehyde as reductant showed the best electrocatalytic activity on the MOR.

There has been massive inert material (active carbon) in the solid phase system, and it prevents the enlargement and aggregation of the Pt particles. Pt (Ⅳ) compound loaded not only on the surface of active carbon, but also in the pores of active carbon. The Pt (Ⅳ) compound on the surface could be reduced by the solid-solid interfacial reaction, but Pt (Ⅳ) compound in pore was hardly reduced. Therefore, the best reductant was the one which can decompose the reductive gas.

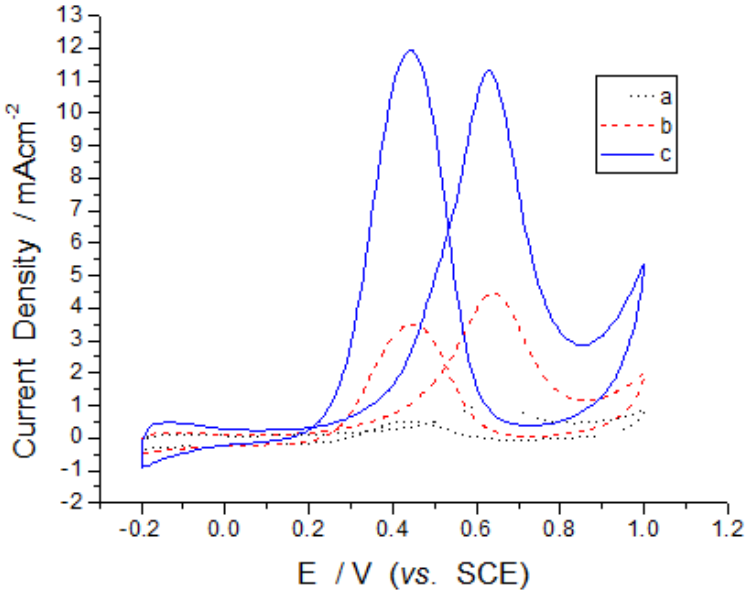

Figure 8. Cyclic voltammograms of the different Pt/C catalysts prepared under the molar ratio of H_2PtCl_6 and NaOH is (a)1:6.4, (b)1:4,(c)1:2. Scan rate 50mV/s.

$NaBH_4$ decomposed easily to generate active hydrogen, so it possessed high reduction performance. But, the quick reaction counted against the generation of ultramicron and made reaction out of control. Meanwhile, using $NaBH_4$ as solid reductant, the generation of large quantity of H_2O caused the quenching of the solid reaction. If sodium formate or sodium citrate was used as solid reductant, the Pt(Ⅳ) compound in the pores of active carbon could not be reduced. Polyformaldehyde was a mild reductant and could decompose to generate active formaldehyde gas under alkaline condition. Therefore, it profited not only the reduction of the Pt(Ⅳ) compound in pore, but also the generation of ultramicron.

The influences of NaOH to the catalyst performance were also investigated. Fig. 8 showed the cyclic voltammetry curves of Pt/C catalyst prepared by solid phase reaction with different NaOH dosage in 0.5 mol L^{-1} CH_3OH +0.5 mol L^{-1} H_2SO_4 solution. As shown, when the molar ratio of H_2PtC1_6 to NaOH was different, the oxidation peak potentials of methanol were the same with different peak currents. When the molar ratio of H_2PtC1_6 to NaOH was 1:6.4 (curve a) with positive

scanning, the peak current was 11.3mA/cm^2. When the molar ratio was 1: 4 (curve b), the peak current was 4.43 mA/cm^2. When the molar ratio was 1: 2 (curve C), the peak current was 1.06 mA/cm^2. When the amount of NaOH is insufficient, the main reason for the lower peak current was that the Pt was not completely reduced and the polyformaldehyde also was not easy to decompose. Obviously, the peak current density increased as the amount of NaOH increased. But, if the amount of NaOH is too much, the reaction would be too violent to control, and resulted in mass loss of activated carbon. The size of the Pt/C catalyst might be attributed to two factors, stereo contraction effect and static charge effect [36]. So, under room temperature, the suitable molar ratio was 1:6.4 (H_2PtCl_6:NaOH).

4. CONCLUSIONS

The Pt/C catalyst was prepared with the SPR method. The results of XRD and TEM showed that it possessed lower crystalline extent and smaller size than that with the LPR method. The electrochemical studies showed that Pt/C catalysts prepared with solid phase reaction method possess higher EAS, and its electrocatalytic activity for methanol oxidation was also higher than that with the LPR method and the same Pt/C catalyst of E-TEK Co. The preparation and electrocatalytic activity of the PtRu/C catalyst with the SPR method was in progress.

ACKNOWLEDGEMENT
This research was supported by the National Natural Science Foundation of China (50972059), Intergovernmental Cooperation Projects in Science and Technology of the Ministry of Science and Technology of PRC (№5) and the Department of Education of Jiangsu Province (CXLX11_0245).

References

1. A. Holdway and O. Inderwildi, *Energy, Transport, & the Environment Addressing the Sustainable Mobility Paradigm*, Springer International Publishing AG, Switzerland (2012)273.
2. J. Fernández-Moreno, G. Guelbenzu, A.J. Martín, M.A. Folgado, P. Ferreira-Aparicio and A.M. Chaparro, *Applied Energy*, 109 (2013) 60.
3. W. Yuan, B. Zhou, J. Deng, Y. Tang, Z. Zhang and Z. Li, *Int. J. Hydrogen Energ*., 39(2014)6689.
4. W. Liu and J. Huang, *J. Power Sources*, 189 (2009) 1012.
5. R. Carrera-Cerritos, R. Fuentes-Ramírez, F.M. Cuevas-Mu~niz, J. Ledesma-García and L.G. Arriaga, *J. Power Sources*, 269 (2014) 370.
6. J.H. Wee, *J. Power Sources*, 173 (2007) 424.
7. J.C. Calderón, G. García, A. Querejeta, F. Alcaide, L. Calvillo, M.J. Lázaro, J.L. Rodríguez and E. Pastor, *Electrochim. Acta*, 186 (2015) 359.
8. L. Zhang, A. Gao, Y. Liu, Y. Wang and J. Ma, *Electrochim. Acta*, 132 (2014) 416.
9. Y.C. Wei, C.W. Liu, W.J. Chang and K.W. Wang, *J. Alloys and Compounds*, 509 (2011) 535.
10. H.Y. Chou, C.K. Hsieh, M.C. Tsai, Y.H. Wei, T.K. Yeh and C.H. Tsai, *Thin Solid Films*, 584 (2015) 98.
11. Y. Takasu, T. Fujiwara, Y. Murakami, K. Sasaki, M. Oguri, T. Asaki and W. Sugimoto, *J. Electrochem. Soc.*, 147 (2000) 4421.
12. Y. Tang, F. Gao, S. Yu, Z. Li and Y. Zhao, *J. Power Sources*, 239 (2013) 374.
13. A. Murthy, E. Lee and A. Manthiram, *Appl.Catal.B:Environ.*, 121– 122 (2012) 154.
14. C. Hu, Y. Cao, L. Yang, Z. Bai, Y. Guo, K. Wang, P. Xu and J. zhou, *Appl. Surf. Sci.*, 257 (2011) 7968.
15. Z. Li, M. Li, M. Han, J. Zeng, Y. Li, Y. Guo and S. Liao, *J. Power Sources*, 268 (2014) 824.

16. P. Kolla and A. Smirnova, *Electrochim. Acta*, 182 (2015) 20.
17. T. Frelink, W. Visscher and J. A. R. van Veen, *J. Electroanal. Chem.*, 382 (1995) 65.
18. B.R. Rauhe, F.R. Mclarnon and E.J. Cairns, *J. Electrochem. Soc*., 142(1995)1073.
19. A.K. Shukla, M.K. Ravikumar, M. Neergat and K.S. Gandhi, *J. Appl. Electrochem.*, 29(1999)129.
20. D.V. Goia and E. Matijevic, *New J. Chem.*, 22 (1998) 1203.
21. A. Stoyanova, V. Naidenov, K. Petrov, I. Nikolov, T. Vitanov and E. Budevski, *J.Appl. Electrochem.*, 29 (1999) 1197.
22. E. Antolini and F. Cardellini, *J. Alloys Compd.*, 315 (2001) 118.
23. A. S. Aricò, P. Cretì, N. Giordano, V. Antonucci, P. L. Antonucci and A. Chuvilin, *J.Appl. Electrochem.*, 26 (1996) 959.
24. W.H. Lizcano-Valbuena, V.A. Paganin, C.A.P. Leite, F. Galembeck and E.R. Gonzalez, *Electrochim. Acta*, 48 (2003) 3869.
25. D.G. Duff, P.P. Edwards and B.F.G. Johnson, *J. Phys. Chem.*, 99 (1995) 15934.
26. T. Teranishi, M. Hosoe, T. Tanaka and M. Miyake, *J. Phys. Chem. B*, 103 (1999) 3818.
27. T. J. Schmidt, H. A. Gasteiger, G. D. Staeb, P. M. Urban, D. M. Kolb and R. J. Behm, *J. Electrochem. Soc.*, 145 (1998) 2354.
28. J. Ma, Y. Tang, G. Yang, Y. Chen, Q. Zhou, T. Lu and J. Zheng, *Appl. Surf. Sci.*, 257 (2011) 6494.
29. K. Lasch, L. Jörissen and J. Garche, *J. Power Sources*, 84 (1999) 225.
30. J. Ma, H. Sun, F. Su, Y. Chen, Y. Tang, T. Lu and J. Zheng, *Int. J. Hydrogen Energ*., 36 (2011) 7265.
31. Y. Takasu, T. Iwazaki, W. Sugimoto and Y. Murakami, *Electrochem. Comm.*, 2 (2000) 671.
32. C. Alegre, D. Sebastián, M. E. Gálvez, R. Moliner, A. Stassi, A. S. Aricò, M. J. Lázaro and V. Baglio, *Catalysts*, 3(2013) 744.
33. E.M. Crabb, R. Marshall and D. Thompsett, *J. Electrochem. Soc.*, 147 (2000) 4440.
34. S. Cui and D. Guo, *J. Colloid Interf. Sci.*, 333 (2009) 300.
35. S. Ang and D. A. Walsh, *J. Power Sources*, 195 (2010) 2557.
36. B. Fang, N. K. Chaudhari, M. Kim, J. H. Kim and J. Yu, *J. Am. Chem. Soc.*, 131(2009) 15330.

© 2016 The Authors. Published by ESG (www.electrochemsci.org). This article is an open access article distributed under the terms and conditions of the Creative Commons Attribution license (http://creativecommons.org/licenses/by/4.0/).